Supporting Information for

Chemical Perturbation of Oncogenic Protein Folding: from the Prediction of Locally Unstable Structures to the Design of Disruptors of Hsp90-Client Interactions

Antonella Paladino,[a,†] Mark R. Woodford,[b,c,d,†] Sarah J. Backe,[b,c,d] Rebecca A. Sager,[b,c,d,e] Priyanka Kancherla,[b,d] Michael A. Daneshvar,[b,d] Victor Z. Chen,[b,c,d] Dimitra Bourboulia,[b,c,d] Elham F. Ahanin,[b,c,d] Chrisostomos Prodromou,[f] Greta Bergamaschi,[a] Alessandro Strada,[a] Marina Cretich,[a] Alessandro Gori,[a] Marina Veronesi,[g] Tiziano Bandiera,[g] Renzo Vanna,[h] Gennady Bratslavsky,[b,c,d] Stefano A. Serapian,[i] Mehdi Mollapour, [b,c,d,*] Giorgio Colombo,[a,i,*]

[a] Drs. A. Paladino, G. Bergamaschi, A. Strada, M. Cretich, A. Gori, G. Colombo*
SCITEC-CNR,
via Mario Bianco 9
20131 Milano, Italy
E-mail: g.colombo@unipv.it

[b,c,d] Drs. M.R. Woodford, S.J. Backe, R.A. Sager, P. Kancherla, M.A. Daneshvar, V.Z. Chen, E.F. Ahain, G. Braslavsky, M. Mollapour*
Department of Urology, SUNY Upstate Medical University Syracuse, NY 13210, USA
Department of Biochemistry and Molecular Biology, SUNY Upstate Medical University Syracuse, NY 13210, USA
Upstate Cancer Center, SUNY Upstate Medical University Syracuse, NY 13210, USA
E-mail: mollapom@upstate.edu

[e] College of Medicine, SUNY Upstate Medical University Syracuse, NY 13210, USA

[f] Dr. C. Prodromou
Genome Damage and Stability Centre,
University of Sussex, Brighton BN1 9RQ, UK

[g] Drs. M. Veronesi, T. Bandiera
D3-PharmaChemistry,
Istituto Italiano di Tecnologia (IIT), Genova, Italy

[i] Prof. Giorgio Colombo*
University of Pavia,
Department of Chemistry
Viale Taramelli 10,
27100 Pavia, Italy
E-mail: g.colombo@unipv.it

† These authors contributed equally to this work

MATERIALS AND METHODS

MD simulations

MD simulations of all proteins described in the main text were carried out using the Gromacs software package (v.4.5.5) (www.gromacs.org) with the Amber99 force field [1]. Selected starting structures for protein kinases were the following: the crystal structures of the active (pdb code 2GQG) and inactive (pdb 2G1T) states of the catalytic domain of c-Abl kinase; the crystal structures of the B-Raf (pdb 4E26), cSrc (pdb 2SRC), and Cdk4 (pdb 3G33). The crystal structure used for the simulation of Glucocorticoid Receptor (GR) was 5nfp.pdb.

All proteins were simulated in their apo forms. The proteins were centered in triclinic boxes allowing a 0.9 nm distance from each box edge and solvated with TIP3P water molecules [2]. Counterions were randomly added to ensure overall charge neutrality. Each system was first energy minimized using the steepest descent approach, followed by a 5 ns simulation in which the positions of the protein heavy atoms were restrained by a harmonic potential. Production trajectories were run for 100 ns at constant temperature of 300 K and a constant pressure of 1 atm [3]. All simulations were run in two independent replicates. A cutoff radius of 0.9 nm for non-bonded van der Waals interactions was used in all simulations. Bond lengths involving hydrogens were restrained by the LINCS algorithm [4]. Electrostatic interactions were treated using the particle mesh Ewald method [5]. The time step was set to 2 fs and periodic boundary conditions were applied in all three dimensions.

Cluster analysis of MD trajectories was performed prior to the prediction of locally unstable structures based on the energy decomposition method [6]. Clustering was carried out using 0.1 nm RMSD cut-off definition for neighbor structures using the method developed by Daura *et al.* [7] The representative structures (centroid) of the first 3 clusters for each system have been analyzed for epitope prediction, and consensus on the predictions on the 3 clusters was used to select the sequences for synthesis.

Computational prediction and design of chaperone/cochaperone targeting regions on client proteins

Prediction of chaperone/cochaperone binding was carried using the MLCE method [6], based on the eigenvalue decomposition of the matrix of residue–residue energy couplings calculated for each client analyzed. Briefly, an interaction matrix M_{ij} is calculated by considering the interaction energies between residue pairs, comprising all the non-bonded inter-residue atomic energy components (namely, van der Waals and electrostatic), in representative clusters of MD trajectory starting from the native conformation. In this calculation, diagonal elements, containing self-interactions, are neglected. The matrix M_{ij} can be diagonalized and re-expressed in terms of eigenvalues and eigenvectors, in the form:

$$M_{ij} = \sum_{k=1}^{N} \lambda_k w_i^k w_j^k \quad (1)$$

where N is the number of amino acids in the protein, λ_k is an eigenvalue, and w_i^k is the *i*-th component of the associated normalized eigenvector. Eigenvalues are labelled following an increasing order, so that λ_1 is the most negative. In the following we refer to the first eigenvector as the eigenvector corresponding to the eigenvalue λ_1. The total non-bonded energy E_{nb} is defined as:

$$E_{nb} = \sum_{i,j=1}^{N} M_{ij} = \sum_{i,j=1}^{N} \sum_{k=1}^{N} \lambda_k w_i^k w^k{}_j \quad (2)$$

If the term $\lambda_k w_i^k w^k{}_j$ for k>1 is smaller than $\lambda_1 w_i^1 w^1{}_j$, each M_{ij} can be approximated by the first contribution only:

$$M_{ij} \approx \tilde{M}_{ij} = \lambda_1 w_i^1 w_j^1 \quad (3)$$

such that the total non bonded energy becomes:

$$E_{nb} \approx E_{nb}^{tot} = \sum_{i,j=1}^{N} \tilde{M}_{ij} = \sum_{i,j=1}^{N} \lambda_1 w_i^1 w_j^1 \quad (4)$$

This simplified energy matrix captures the residue pairs contributing most to the stabilization of the overall fold [12c, 12g, 14d-f, 31], as well as the structures that are unstable and prone to support the local, large structural fluctuations that lead to unfolding. To focus on the latter, the map of pair energy-couplings corresponding to the lowest eigenvector is filtered with the contact matrix, to identify which local couplings characterized by energetic interactions of minimal intensities. Thanks to the low intensity constraints to the rest of the protein, these substructures would be characterized by dynamic properties that allow them to visit multiple conformations, a subset of which can be lead to local unfolding and be recognized by members of the Hsp90 chaperone system. The lowest 15% of all contact-filtered pairs define the residue making up the predicted chaperone/cochaperone binding sequences.

Synthesis of peptide-based mimics of client interaction substructures

Peptides spanning the predicted chaperone-interaction regions of the client proteins studied here were synthesized with classical solid-phase based methods. See Supplementary Information for details.

NMR Experiments

All the NMR experiments have been recorded at 298°K with a Bruker FT NMR Avance III 600-MHz spectrometer equipped with a 5-mm CryoProbe™ QCI ^{1}H/^{19}F-^{13}C/^{15}N-D quadruple resonance, a shielded z-gradient coil, and the automatic sample handling system SampleJet™ with temperature control.

^{19}F NMR experiments are nowadays a well-recognized approach to study the interaction between small molecules or peptides and proteins[8]. ^{19}F NMR shows one of the largest relative sensitivity to protein binding events. This is due to the large dynamic range, defined

as the difference of the NMR measured response in the free and protein-bound states. ^{19}F R_2 filter NMR experiments are among the most sensitive techniques for weak binding detection[9]. The transverse relaxation rate R_2 is a very sensitive parameter for these studies, due to the large Chemical Shift Anisotropy (CSA) of ^{19}F nucleus and to the large exchange contribution [10]: the compounds/peptides that interact with the receptor will show a broadening and intensity reduction in their ^{19}F NMR signal in presence of the protein

The 5 mM stock solution peptides were prepared in 100% in DMSO*d6*. Solubility and purity of the peptides in PBS buffer pH 7.4, 10% D_2O (for the lock signal) were checked by ^{19}F and ^{1}H NMR spectroscopy. 1D ^{19}F NMR experiments were recorded with proton decoupling with the Waltz-16 scheme during the acquisition period with an acquisition time of 0.95 s, a relaxation delay of 30 s. whereas 1D version of the NOESY (nuclear Overhauser effect spectroscopy) pulse sequence with H_2O signal presaturation, a mixing time of 10 ms and a relaxation delay of 30 s was used for ^{1}H NMR experiments.

For the binding studies R_2 filter experiments were recorded with the Carr-Purcell-Meibom-Gill scheme with a time interval of 23.5 ms between the 180° pulses with a loop of 2, an acquisition time of 0.95s a D1 of 5s and a number of scans of 512.

All the 19F chemical shifts are referenced to the $CFCl_3$ signal in water.

Mammalian Cell Culture

Human embryonic kidney (HEK293) and 786-O cells were acquired from the American Type Culture Collection (ATCC). HEK293 cells were grown in Dulbecco's Modified Eagle Medium (DMEM, Millipore-Sigma) and 786-O cells were grown in Roswell Park Memorial Institute (RPMI-1640, Millipore-Sigma) medium supplemented with 10% fetal bovine serum (FBS, Millipore-Sigma) in a CellQ incubator (Panasonic Healthcare) at 37° C in 5% CO_2.

Peptide Treatment

Cultured cells were seeded 24h prior to treatment. Peptides were added to cells at 50% confluency at the indicated concentrations and incubated for 24h, followed by protein extraction as described below.

Protein Extraction, Immunoprecipitation and Immunoblotting

Protein extraction from mammalian cells was carried out using methods previously described [11]. For immunoprecipitation, protein lysates were incubated with Hsp90 antibody for 2h followed by incubation with protein G agarose (Qiagen) for 2h at 4° C. Immunopellets were washed 4 times with fresh lysis buffer (20mM Tris (pH7.4), 100mM NaCl, 1 mM MgCl2, 0.1% NP40, protease inhibitor cocktail (Roche), and PhosSTOP (Roche)) and eluted with 5x Laemmli buffer. Precipitated proteins were separated by SDS-PAGE and transferred to nitrocellulose membranes. Co-immunoprecipitated proteins were detected by immunoblotting with the indicated antibodies, diluted in 5% non-fat dry milk reconstituted in TBST.

Biotinylated Peptide Pulldown

Total cell lysates prepared as described above were incubated with the indicated amounts of biotinylated peptide at 4°C for 1h. Streptavidin agarose beads (ThermoScientific) were added and incubated 1 additional hour with gentle rotation. Bound Hsp90 was detected by immunoblotting as described above.

Fluorescence Imaging

FAM-labeled peptides were incubated with cultured cells for 24h. Brightfield and fluorescent images were captured using the ZOE Fluorescent Cell Imager (Bio-Rad).

Peptide synthesis and characterization

Materials

HMPB resin, *N*-α-Fmoc-L-amino acids and building blocks used during chain assembly were purchased from Iris Biotech GmbH (Marktredwitz, Germany). Ethyl cyanoglyoxylate-2-oxime (Oxyma) was purchased from Novabiochem (Darmstadt, Germany), *N,N'*-dimethylformamide (DMF) and trifluoroacetic acid (TFA) were from Carlo Erba (Rodano, Italy). N,N'-diisopropylcarbodiimide (DIC), dichloromethane (DCM) and all other organic reagents and solvents, unless stated otherwise, were purchased in high purity from Sigma-Aldrich (Steinheim, Germany). All solvents for solid-phase peptide synthesis (SPPS) were used without further purification. HPLC grade acetonitrile (ACN) and ultrapure 18.2 Ω water (Millipore-MilliQ) were used for the preparation of all buffers for liquid chromatography. The chromatographic columns were from Phenomenex (Torrance CA, USA). HPLC eluent A: 97.5% H_2O, 2.5% ACN, 0.7%TFA; HPLC eluent B: 30% H_2O, 70% ACN, 0.7%TFA

Peptide Synthesis: General Procedures

Resin loading

Resin (0.5 mmol/g loading) was swollen in CH_2Cl_2 for 30 min then washed with DMF (3 × 3 mL). A solution of entering Fmoc- amino acid, DIC and Oxyme (5:5, 5 eq over resin loading) and 5% of DMAP in DMF (3 mL) was added and the resin shaken at rt for 4 h. The resin was washed with DMF (2 × 3 mL) and capping was performed by treatment with acetic anhydride/ DIEA in DCM (1 x 30 min). The resin was then washed with DMF (2 × 3 mL), CH_2Cl_2 (2 × 3 mL), and DMF (2 × 3 mL). The resin was subsequently submitted to fully automated iterative peptide assembly (Fmoc-SPPS).

Peptide Assembly via Iterative Fully Automated Microwave Assisted SPPS

Peptides were assembled by stepwise microwave-assisted Fmoc-SPPS on a Biotage ALSTRA Initiator+ peptide synthesizer, operating in a 0.1 mmol scale. Activation of entering Fmoc-protected amino acids (0.3M solution in DMF) was performed using 0.5M Oxyma in DMF / 0.5M DIC in DMF (1:1:1 molar ratio), with a 5 equivalent excess over the initial resin loading. Coupling steps were performed for 7 minutes at 75°C. Fmoc- deprotection steps were performed by treatment with a 20% piperidine solution in DMF at room temperature (1 x 10 min). Following each coupling or deprotection step, peptidyl-resin was washed with

DMF (4 x 3.5 mL). Upon complete chain assembly, resin was washed with DCM (5 x 3.5 mL) and gently dried under a nitrogen flow.

Cleavage from the Resin

Resin-bound peptide was treated with an ice-cold TFA, TIS, water, thioanisole mixture (90:5:2.5:2.5 v/v/v/v, 4mL). After gently shaking the resin for 2 hours at room temperature, the resin was filtered and washed with neat TFA (2 x 4 mL). The combined cleavage solutions were worked-up as indicated below.

Work-up and Purification

Cleavage mixture was concentrated under nitrogen stream and then added dropwise to ice-cold diethyl ether (40 mL) to precipitate the crude peptide. The crude peptide was collected by centrifugation and washed with further cold diethyl ether to remove scavengers. Residual diethyl ether was removed by a gentle nitrogen flow and the crude peptide was purified by RP-HPLC and lyophilized.

Synthesis of Fluorescein-labelled peptides

Cysteine-bearing peptides were conjugated to bifunctional MAL-FAM (Lumiprobe GmbH, Germany) as follows: peptide (1 eq.) was dissolved in phosphate buffer (Na_2HPO_4 0.4M, pH 7.8). The resulting solution was ice-cooled and mixed with MAL-FAM solution (1.2 eq., 50:50 acetonitrile/water mixture). The reaction mixture was left to react for under gentle shaking until full reagents conversion (RP-HPLC monitoring). Upon reaction completion, conjugation products were isolated by preparative RP-HPLC and lyophilized.

RP-HPLC analysis and purification

Analytical RP-HPLC was performed on a Shimadzu Prominence HPLC (Shimadzu) using a Shimadzu Shimpack GWS C18 column (5 micron, 4.6 mm i.d. x 150 mm). Analytes were eluted using a binary gradient of mobile phase A (100% water, 0.1% trifluoroacetic acid) and mobile phase B (30% water, 70% acetonitrile, 0.1% trifluoroacetic) using the following chromatographic method: 10% B to 100% B in 14 min; flow rate, 1 ml/min.

Preparative RP-HPLC was performed on a Shimadzu HPLC system using a Shimadzu C18 column (10 micron, 21.2 mm i.d. x 250 mm) using the following chromatographic method: 0% B to 100% B in 45 min; flow rate, 14 ml/min. Pure RP-HPLC fractions (>95%) were combined and lyophilized.

Electro-spray ionization mass spectrometry (ESI-MS)

Electro-spray ionization mass spectrometry (ESI-MS) was performed using a Bruker Esquire 3000+ instrument equipped with an electro-spray ionization source and a quadrupole ion trap detector (QITD).

Table S1: Peptide list

Code	Sequence
A01	LGGGQ**F(F)**GEVYGGVAVKTLGGGEFLDEAAVMK
A02	**F(F)**GGSPYPGIDLSQVYELLEK
B-Raf_01	GYSTKPQLAGGGNVTAPTPQG**F(F)**QHSGS
B-Raf_01	FGTVYKGKWGGGG**F(F)**STKPQLAGGGNVTAPTPQ
Cdk4_01	CATSRTDREGPNGGGGGGGLPISTGG**F(F)**QMALTPVV
Cdk4_02	PVAEIGVGAYGGGRVPGG**F(F)**QMALTPVV
cSrc_01	LGQGC**F(F)**GGKPGTMSPGGEEPGGRESLGWNGTT
cSrc_02	GEMGKGGKGRVPYPGMVNREVLDQVERG**F(F)**RM
GR-01	TLPCGGTWRIMTGIE **F(F)**PEMLA
GR-02	YAGYDSSVPDSTWRIMTTLNMGG**F(F)**PEMLA

F(F) = 4-Fluoro-L-phenylalanine

Table S2: Peptide characterization

Code	ESI-MS (m/z) found	ESI-MS (m/z) calculated	Rt
A01	1031.3 (M^{3+}), 1546.9 (M^{2+})	1031.2 (M^{3+}), 1546.3 (M^{2+})	11.2 min
A02	1116.2 (M^{2+})	1116.7 (M^{2+})	12.05 min
B-Raf_01	1303.7 (M^{2+})	1303.5 (M^{2+})	8.3 min
B-Raf_02	1592.9 (M^{2+}), 1062.3 (M^{3+})	1593.7 (M^{2+}), 1062.8 (M^{3+})	9.1 min
Cdk4_01	1677.9 (M^{2+})	1677.8 (M^{2+})	9.8 min
Cdk4_02	2634.5 (M^{+}), 1318.0 (M^{2+})	2634.2 (M^{+}), 1317.7 (M^{2+})	11.7 min
cSrc_01	1579.1 (M^{2+}), 1052.8 (M^{3+})	1579.5 (M^{2+}), 1053 (M^{3+})	8.9 min
cSrc_02	1735.3 (M^{2+}), 1157.3 (M^{3+})	1735.1 (M^{2+}), 1157.1 (M^{3+}),	10.1 min
GR01	1172.6 (M^{2+})	1172.3 (M^{2+})	12.56 min
GR02	1116.5 (M^{2+})	1116.3 (M^{2+})	12.52 min
B-Raf_01 _FAM	1070.5 (M^{3+}), 1605.2 (M^{2+})	1070.3 (M^{3+}), 1604.8 (M^{2+})	9.9 min
B-Raf_02_FAM	1263.1 (M^{3+}), 1895.0 (M^{2+})	1894.8.5 (M^{2+}), 1263.5 (M^{3+})	10.4 min
Cdk4_01_FAM	1925.4 (M^{2+}), 1284.7 (M^{3+}),	1925.5 (M^{2+}), 1284.5 (M^{3+})	11.2 min
Cdk4_02_FAM	1618.5 (M^{2+})	1618.6 (M^{2+})	12.1 min
cSrc_01 _FAM	1419.3 (M^{3+}), 1064.8 (M^{4+})	1419.6 (M^{3+}), 1065 (M^{4+})	11.3 min
cSrc_02_FAM	1373.7 (M^{3+}), 1030.9 (M^{4+})	1373.6 (M^{3+}), 1030.5 (M^{4+})	11.9 min

Figure S1. ^{19}F NMR experiments to check the binding of Abl and Braf peptides to HSA. (a) Peptide Abl01; (b) Abl02-pep; (c) Braf01-pep; (d) Braf02-pep; No peptide shows a significant difference in their ^{19}F signals in presence of protein, indicating that they do not interact with HSA.

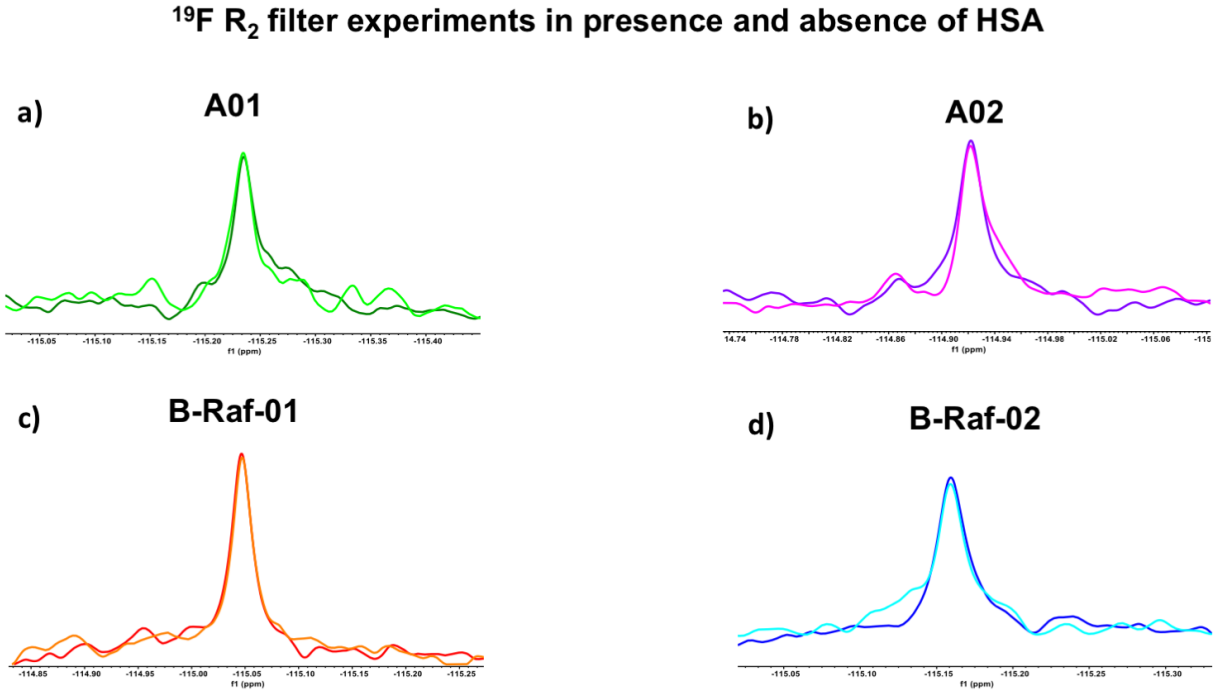

Figure S2. ^{19}F NMR experiments to check the purity of synthesized peptides.

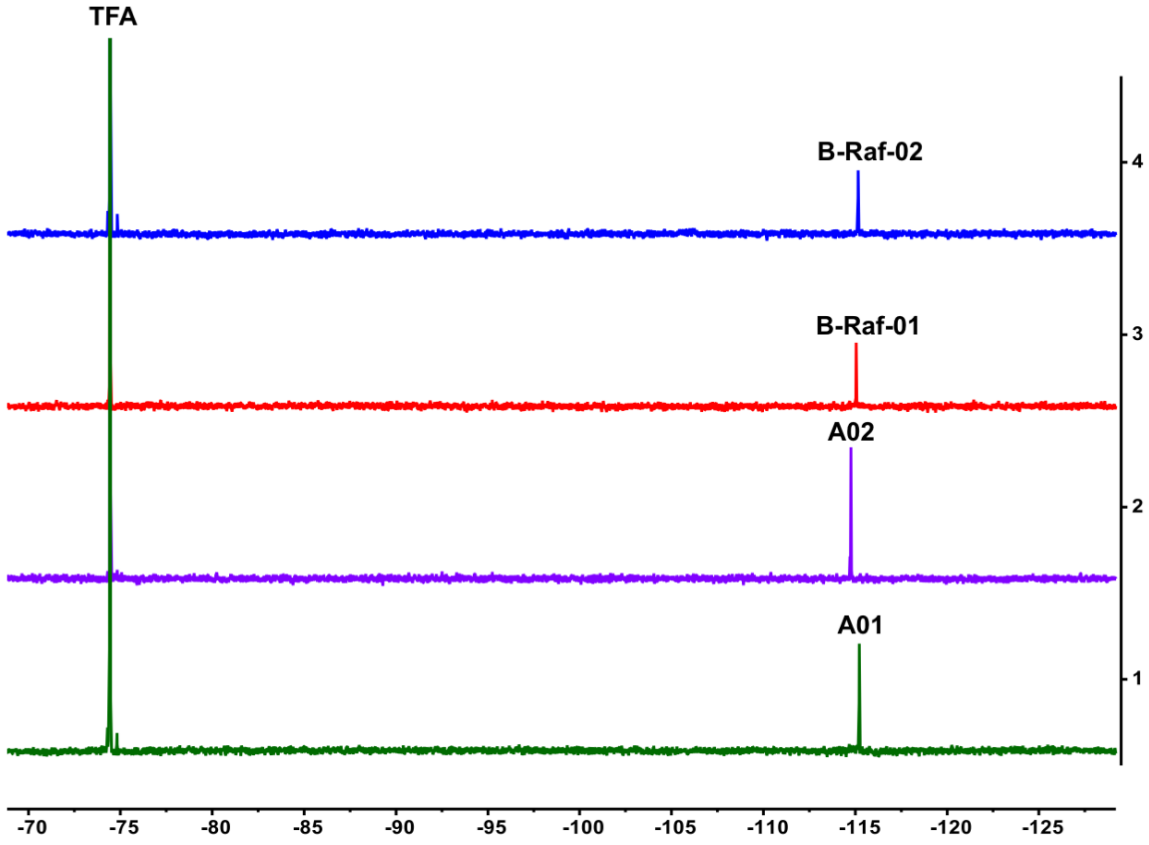

Figure S3. ^{19}F NMR experiments to check the stability of synthesized peptides in TRIS buffer

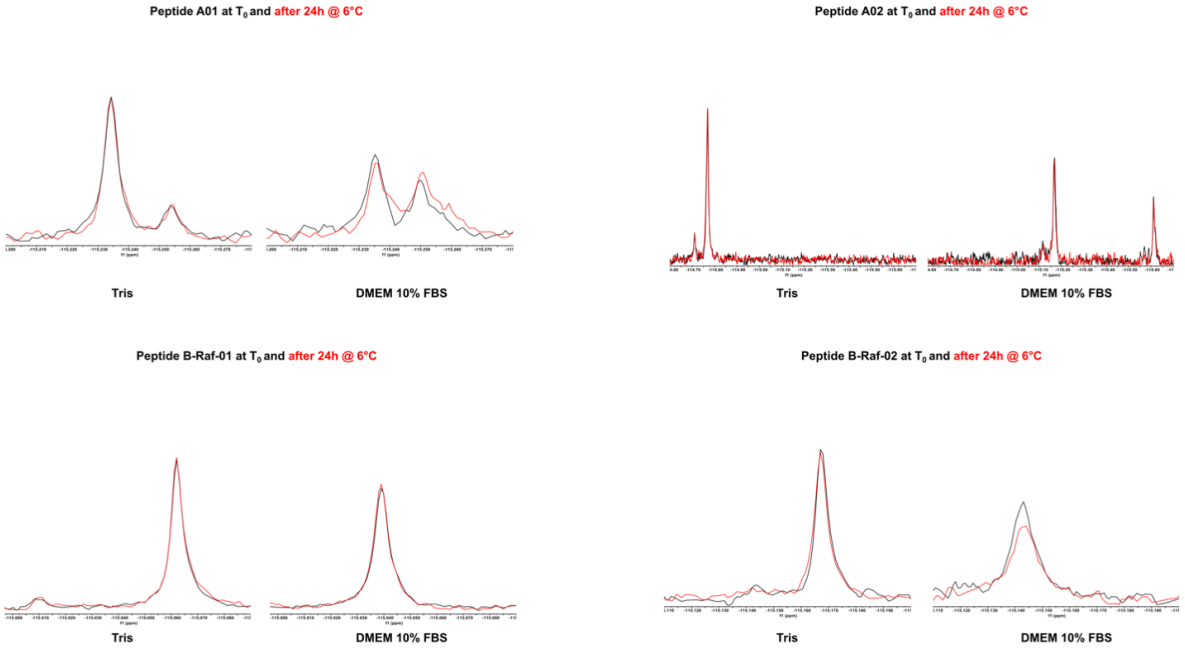

References

[1] D. A. Case, D. S. Cerutti, T. E. I. Cheatham, T. A. Darden, R. E. Duke, T. J. Giese, H. Gohlke, A. W. Goetz, D. Greene, N. Homeyer, S. Izadi, A. Kovalenko, T. S. Lee, S. LeGrand, P. L. Li, C. , J. Liu, T. Luchko, R. Luo, D. Mermelstein, K. M. Merz, G. Monard, H. Nguyen, I. Omelyan, A. Onufriev, F. Pan, R. Qi, D. R. Roe, A. Roitberg, C. Sagui, C. L. Simmerling, W. M. Botello-Smith, J. Swails, R. C. Walker, J. Wang, R. M. Wolf, X. Wu, L. Xiao, D. M. York, P. A. Kollman, *University of California, San Francisco* **2017**.

[2] W. L. Jorgensen, J. Chandrasekhar, J. Madura, R. W. Impey, M. L. Klein, *J. Chem. Phys.* **1983**, *79*, 926-935.

[3] H. J. C. Berendsen, J. P. M. Postma, W. F. van Gunsteren, A. Di Nola, J. R. Haak, *J. Chem. Phys.* **1984**, *81*, 3684-3690.

[4] B. Hess, H. Bekker, J. G. E. M. Fraaije, H. J. C. Berendsen, *J.Comp.Chem.* **1997**, *18*, 1463-1472.

[5] T. Darden, D. York, L. Pedersen, *J. Chem. Phys.* **1993**, *98*.

[6] a) F. Marchetti, R. Capelli, F. Rizzato, A. Laio, G. Colombo, *J. Phys. Chem. Lett.* **2019**, *10*, 1489-1497; b) C. Peri, P. Gagni, F. Combi, A. Gori, M. Chiari, R. Longhi, M. Cretich, G. Colombo, *ACS Chemical Biology* **2013**, *8*, 397-404 ; c) G. Morra, G. Colombo, *Proteins: Struct. Funct. and Bioinf.* **2008**, *72*, 660-672; d) G. Scarabelli, G. Morra, G. Colombo, *Biophys. J.* **2010**, *98*, 1966-1975; e) A. Genoni, G. Morra, G. Colombo, *J. Phys. Chem. B.* **2012**, *116*, 3331-3343.

[7] X. Daura, K. Gademann, B. Jaun, D. Seebach, W. F. v. Gunsteren, A. E. Mark, *Angew. Chemie Intl. Ed.* **1999**, *38*, 236-240.

[8] C. Dalvit, A. Vulpetti, *J. Med. Chem.* **2018**, *62*, 2218-2244.

[9] C. Dalvit, *Drug Discov. Today* **2009**, *14*, 1051-1057.

[10] C. Dalvit, P. E. Fagerness, D. T. A. Hadden, R. W. Sarver, B. J. Stockman, *Journal of the American Chemical Society* **2003**, *125*, 7696-7703.

[11] M. R. Woodford, A. W. Truman, D. M. Dunn, S. M. Jensen, R. Cotran, R. Bullard, M. Abouelleil, K. Beebe, D. Wolfgeher, S. Wierzbicki, D. E. Post, T. Caza, S. Tsutsumi, B. Panaretou, S. J. Kron, J. B. Trepel, S. Landas, C. Prodromou, O. Shapiro, W. G. Stetler-Stevenson, D. Bourboulia, L. Neckers, G. Bratslavsky, M. Mollapour, *Cell Reports* **2016**, *14*, 872-884.